DOI: 10.1007/s11099-018-0765-0 PHOTOSYNTHETICA 56 (1): 192-199, 2018

Regulating photoprotection improves photosynthetic growth and biomass production in Q_C-site mutant cells of the cyanobacterium *Synechocystis* sp. PCC 6803

J.-Y. HUANG, N.-T. HUNG, K.-M. LIN, Y.-F. CHIU, and H.-A. CHU+

Institute of Plant and Microbial Biology, Academia Sinica, Taipei, 11529, Taiwan

Abstract

We characterized the photosynthetic growth of wild-type (WT) and Q_C-site mutant cells of the cyanobacterium *Synechocystis* sp. PCC 6803 grown in a photobioreactor under medium-intensity [~70 μmol(photon) m^{-2} s^{-1}] and high-intensity [~200 μmol(photon) m^{-2} s^{-1}] light conditions. Photosynthetic growth rate (the exponential phase) increased about 1.1–1.2 fold for the A16FJ, S28Aβ, and V32Fβ mutant compared with WT cells under medium-intensity light and about 1.2–1.3 fold under high-intensity light. Biomass production increased about 17–20% for A16FJ and S28Aβ mutant cells as compared with WT cells under medium-intensity light and about 14–17% for A16FJ and V32Fβ mutant cells under high-intensity light. The greater photosynthetic growth rate and biomass production of these Q_C-site mutant cells could be attributed to the increased photosynthesis efficiency and decreased dissipation of wasteful energy from phycobilisomes in mutants *vs*. WT cells. Our results support that manipulation of photoprotection may improve photosynthesis and biomass production of photosynthetic organisms.

Additional key words: cytochrome b_{559}; photosynthesis; photosystem II; photoprotection; Q_C.

Introduction

Cyanobacteria have developed short-term light adaption mechanisms to regulate excitation energy transfer from the antenna complex (phycobilisome) to the photosystems to optimize photosynthesis efficiency and to protect the photosynthetic apparatus against photodamage. The two major mechanisms are state transitions (Bruce *et al.* 1989, Mullineaux and Allen 1990, Kondo *et al.* 2009) and orange carotenoid protein (OCP)-related nonphotochemical fluorescence quenching (NPQ) (Wilson *et al.* 2006, Kirilovsky 2015, Kirilovsky and Kerfeld 2016).

The state transition mechanism in cyanobacteria regulates the distribution of excitation energy from the phycobilisome to the two photosystems depending on changes in the redox state of the plastoquinone (PQ) pool by illumination conditions (Bruce *et al*. 1989, Mullineaux and Allen 1990, Kondo *et al*. 2009). In cyanobacteria, state 1, which enhances excitation energy transfer from the phycobilisome to PSII over PSI, is triggered by an oxidized PQ pool (induced by blue or far-red light), whereas state 2, which enhances excitation energy transfer to PSI over PSII, is triggered by a reduced PQ pool (induced by orange light or dark adaptation). In addition, state transitions in cyanobacteria may involve relative movements between phycobilisome and/or photosystems, but the molecular mechanism is unclear (Kirilovsky 2015).

The OCP-related NPQ mechanism occurs in many cyanobacteria including the cyanobacterium *Synechocystis* sp. PCC 6803 (Wilson *et al*. 2006, Kirilovsky 2015, Kirilovsky and Kerfeld 2016). On absorbing blue-green light, the OCP undergoes conformational changes into the active red form, which interacts with the allophycocyanin core of the phycobilisome to induce the NPQ effect (dissipate excess light energy as heat) and thereby protect PSII reaction centers against photodamage. When blue-green (or white) light intensity is diminished, the red form of OCP is deactivated and released from the phycobilisome by the action of the fluorescence recovery protein, which stops the NPQ effect (Boulay *et al.* 2010).

Received 29 April 2017, *accepted* 5 September 2017, *published as online-first* 10 January 2018.
+Corresponding author; phone: 886-2-27871169, fax: 886-2-27827954, e-mail: chuha@gate.sinica.edu.tw.
Abbreviations: Chl – chlorophyll; Cyt – cytochrome; F_m – the maximal fluorescence yield; $F_{m,dark}$ – the maximal fluorescence yield in the dark; F_0 – the dark fluorescence yield; HP – high- potential form; IP – intermedium potential form; LP – low-potential form; NPQ – nonphotochemical fluorescence quenching; OCP – orange carotenoid proteins; PQ – plastoquinone; WT – wild-type control *Synechocystis* strain constructed in the same manner as site-directed mutants but with no mutation.
Acknowledgments: This work was supported by the Ministry of Science and Technology, Taiwan (MOST 105-2311-B-001-053) and Academia Sinica (to H.A. Chu).

A novel PQ molecule (Q_C) and its diffusion channel were discovered in the 2.9-Å resolution X-ray crystallographic structure model of PSII for the cyanobacterium *Thermosynechococcus elongatus* (Guskov *et al.* 2009, Müh *et al.* 2012). The head group of the Q_C molecule, situated in a hydrophobic environment, is constituted by the tails of lipids, Q_B, and a carotenoid molecule; the Q_C tail locates in a hydrophobic cavity surrounded by the transmembrane helixes of cytochrome (Cyt) b_{559} α and β subunits and PsbJ, which is connected to the internal space of the thylakoid membranes. The Q_C site was proposed to function in exchange of PQ/PQH_2 on the Q_B site from the pool (Kaminskaya *et al.* 2007a,b) or to modulate the redox potential and reactivity of Cyt b_{559} (Kruk and Strzałka 1999, 2001; Bondarava *et al.* 2003, Guskov *et al.* 2009, Müh *et al.* 2012, Kaminskaya and Shuvalov 2013). However, recent high-resolution crystal structure models of PSII from *T. vulcanus* showed no occupancy of PQ on the Q_C site (Umena *et al.* 2011, Suga *et al.* 2015), possibly because of a loose binding of PQ to the Q_C site (Hasegawa and Noguchi 2014). The function of the Q_C site is still unclear.

To reveal the physiological function of the Q_C site in PSII, several Cyt b_{559} and PsbJ mutant cells with mutations on and near the Q_C site and near the opening of the proposed Q_C transfer channel in PSII were constructed and characterized in *Synechocystis* sp. PCC 6803 (Huang *et al.* 2016). Several Q_C-site mutant cells (*e.g.*, A16FJ, S28Aβ, and V32Fβ) showed a greater increase in PSII fluorescence yield than wild-type (WT) cells under medium-intensity blue-light illumination because of enhanced transition from state 2 to 1. In addition, these Q_C-site mutant cells showed weakened effects of OCP-mediated NPQ under strong blue-light illumination (Huang *et al.* 2016). The results suggest that the mutations on the Q_C site of PSII may modulate short-term light adaptations of the photosynthetic apparatus (state transition and OCP-mediated NPQ) in *Synechocystis* sp. PCC 6803. In addition, these Q_C-site mutant cells (A16FJ, S28Aβ, and V32Fβ) showed greater photosynthetic growth and biomass production (about 1.1-fold and 30–40%, respectively) than that of WT cells under normal growth conditions [continuous illumination at ~30 μmol(photon) m^{-2} s^{-1} and 30°C]. The improved photosynthesis and growth characteristics of these mutant cyanobacteria are intriguing because of their potential applications in enhancing the production of biofuels or valuable bioproducts of cyanobacteria.

In this work, in order to test whether these Q_C-site mutant cells show improved photosynthesis under different light conditions, we characterized the photosynthetic growth and biomass production of WT and Q_C-site mutant cells grown in a photobioreactor under both medium- and high-intensity light conditions. In addition, we characterized the redox properties of Cyt b_{559} in WT and Q_C-site mutant PSII core complexes. We discussed the potential applications of mutant cyanobacteria for enhancing the production of biofuels or valuable bioproducts of cyanobacteria.

Materials and methods

Growth and preparation of *Synechocystis* sp. PCC 6803 cells: WT and mutant *Synechocystis* sp. PCC 6803 cells were grown photoautotrophically in BG-11 medium in a growth chamber or photobioreactor (*Multi-Cultivator MC 1000-OD*, *Photon Systems Instruments*, Czech Republic) at 30°C under the light intensity conditions described in the figure legends. The construction of WT and mutant strains has been previously described (Huang *et al.* 2016). Cultures were continuously bubbled with sterile humidified air. Liquid cultures in exponential growth (OD_{730}: 0.7–1.2) were harvested and used for chlorophyll (Chl) fluorescence and functional analysis.

Biomass determination: An amount of 50 ml of culture in the photobioreactor was harvested after 120 h and concentrated to about 5 ml by centrifugation, then oven-dried in aluminium dishes for 24 h at 105°C. After being cooled to room temperature, dry mass was determined (Page *et al.* 2012, Huang *et al.* 2016).

Chl *a* fluorescence measurements at 22ºC involved a dual pulse-amplitude-modulation (PAM) fluorometer (*Walz*, Germany). An amount of 16 μg(Chl) of WT or mutant cells was diluted into BG-11 medium (to a total volume of 1.6 mL), held at 22°C in a stirred, water-jacketed cell and dark-adapted for 5 min. Time-dependent flash-induced transients of PSII fluorescence yield were recorded by using the automated Induction and Recovery Curve routine provided by the *DualPAM* software.

Preparation of His-tagged PSII core complexes: Oxygen-evolving His-tagged PSII core complexes were isolated from WT and mutant cells containing a His-tag on their CP47 proteins by using nickel-nitrilotriacetic acid affinity chromatography as described by Hung *et al.* (2010).

Reduced minus oxidized difference spectra of Cyt b_{559} in WT and mutant PSII core complexes: Optical absorption difference was measured in suspensions of WT and mutant PSII core complexes [20 μg(Chl) mL^{-1}] in 1 mL of MMNB buffer (25 mM MES, 5 mM $MgCl_2$, 10 mM NaCl, 1 M glycine betaine, 0.03% β-DM, pH 5.7) at room temperature, on a *Perkin Elmer Lambda 35* UV/VIS spectrophotometer, with band width 0.5 nm. Four-step redox titration was performed as described by Chiu *et al.* (2013). The sample suspension was oxidized by adding 0.1 mM $K_3Fe(CN)_6$ (from a freshly made 10 mM stock solution), and the spectrum was recorded and stored as the oxidized spectrum. The sequential reduction of cytochromes

involved first adding hydroquinone (0.3 mM), followed by ascorbate (0.6 mM) and finally 2.5 mM dithionite (from a freshly made 500 mM stock solution).

Photosynthetic oxygen evolution: Steady-state rates of oxygen evolution were measured by using a Clark-type oxygen electrode (*YSI model 5331* oxygen probe, USA) fitted with a water-jacketed cell. An amount of 20 μg(Chl) of WT or mutant PSII core complexes was diluted into the oxygen assay buffer (1 M sucrose, 50 mM MES, 25 mM $CaCl_2$, 10 mM NaCl, pH 6.5) held at 25°C in a stirred, water-jacketed cell. Amounts of 1 mM potassium ferricyanide and 0.4 mM 2,6-dichloro-*p*-benzoquinone were added as an artificial electron acceptor into the oxygen assay buffer (to a total volume of 1.6 mL) (Chiu *et al.* 2013). Saturating illumination was provided from both sides of the water-jacketed cell by two fiber-optic illuminators (*Dolan-Jenner model MI 150*, USA).

Results

Photosynthetic growth rate and biomass production of Q_C-site mutant cells: Fig. 1 shows the photosynthetic growth curves for WT, A16FJ, S28Aβ, and V32Fβ mutant cells grown in the photobioreactor under white-LED-light illumination at medium intensity [~70 μmol(photon) m^{-2} s^{-1}] and high intensity [~200 μmol(photon) m^{-2} s^{-1}]. Photosynthetic growth rate (the exponential phase) was greater for A16FJ, S28Aβ, and V32Fβ mutant than that of WT cells under both light conditions (Fig. 1, Table 1). The doubling time of the exponential phase growth rate was 9.5, 8.1, 7.7, and 8.4 h for the WT, A16FJ, S28Aβ, and V32Fβ mutant cells under medium-intensity light, respectively, and 9.8, 7.8, 7.8, and 7.6 h under high-intensity light, respectively (Table 1). After the exponential phase, photosynthetic growth of S28Aβ mutant cells was significantly slower than that of WT and other mutant cells possibly because of photoinhibition under high-intensity light. In addition, biomass concentration calculated for 5-d cultures of A16FJ, S28Aβ, and V32Fβ mutant cells was about 1.17-, 1.20-, and 1.02-fold higher, respectively, than for WT cells under medium-intensity light and about 1.14-, 0.95-, and 1.17-fold under high-intensity light, respectively (Table 1). Therefore, biomass production significantly increased in A16FJ and S28Aβ mutant cells under medium-intensity light and in A16FJ and V32Fβ mutant cells under high-intensity light as compared with WT cells. Furthermore, photosynthetic growth rates and biomass production of WT and most mutant cells showed little or no increase under high- than medium-intensity light [~200 *vs.* ~70 μmol(photon) m^{-2} s^{-1}]. Our results suggested that under ~200 μmol(photon) m^{-2} s^{-1} light, a large portion of light energy was not utilized by mutant and WT cells for photosynthetic growth but likely dissipated as heat *via* the NPQ effect.

PSII fluorescence yield in the presence and absence of blue actinic light: Fig. 2 shows the changes in time-dependent flash-induced PSII fluorescence yield for WT and mutant cells under low-intensity blue actinic light [~30 μmol(photon) m^{-2} s^{-1}] followed by a period of recovery without actinic light. WT and mutant cultures were propagated in the bioreactor under continuous illumination of white-LED light at ~70 μmol(photon) m^{-2} s^{-1}. In cyanobacteria, dark conditions induce the state 2. With ~30 μmol(photon) m^{-2} s^{-1} blue actinic light, the increase in PSII fluorescence yield (due to the transition to the state 1) was greater in A16FJ, S28Aβ, and V32Fβ mutant cells (Fig. 2*B–D*) than that of WT cells (Fig. 2*A*). With ~250 μmol(photon) m^{-2} s^{-1} blue actinic light, WT cells showed a strong quenching in PSII fluorescence yield (Fig. 3*A*). In contrast, A16FJ, S28Aβ, and V32Fβ mutant cells showed

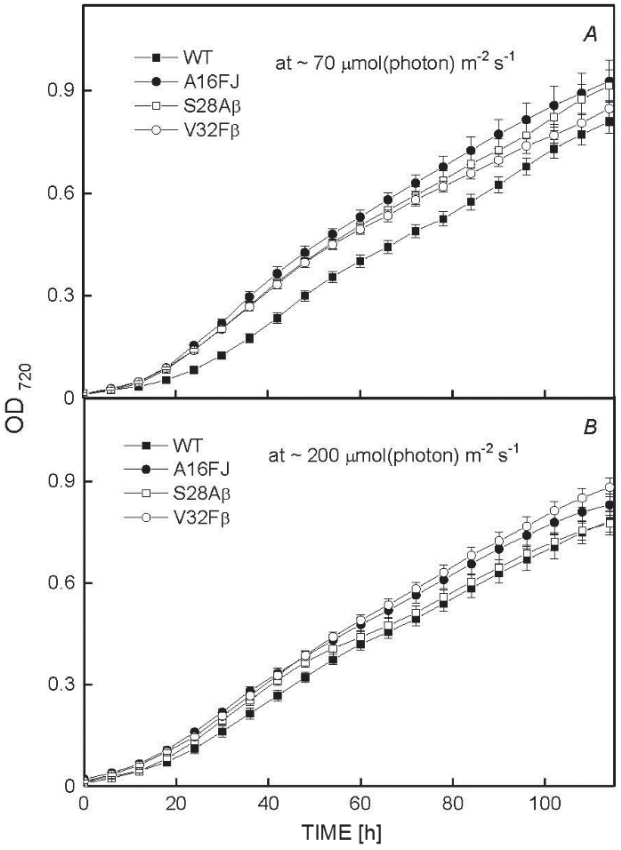

Fig. 1. Photosynthetic growth curves for wild-type (WT) and Q_C-site mutant cells of the cyanobacterium *Synechocystis* sp. PCC 6803 grown in the *Multi-Cultivator MC 1000-OD* photobioreactor under medium-intensity light [~70 μmol(photon) m^{-2} s^{-1}] (*A*) and high-intensity light [~200 μmol(photon) m^{-2} s^{-1}] (*B*) (continued illumination with white LED light). The photosynthetic growth of the cultures was monitored by optical density 720 nm (OD_{720}) which measures light scattering. Data are mean ± SE of 3–5 independent experiments.

Table 1. Photosynthetic growth rates and biomass production in wild-type (WT) and A16FJ, S28Aβ, and V32Fβ Q_C-site mutant cells of the cyanobacterium *Synechocystis* sp. PCC 6803. Cultures were grown in a photobioreactor at 30°C in ambient air and under continuous illumination [~70 or ~200 μmol(photon) m^{-2} s^{-1}]. Photosynthetic growth rates were measured in the exponential phase of growth. Biomass concentrations of cultures were measured after about 120 h of growth. Data are mean ± SE from three independent experiments.

Light intensity [μmol(photon) m^{-2} s^{-1}]	Strain	Doubling time [h]	Biomass concentration [mg mL^{-1}] (fold biomass of WT)
70	WT	9.5 ± 1.0	0.59 ± 0.04
	A16FJ	8.1 ± 0.3	0.69 ± 0.08 (1.17)
	S28Aβ	7.7 ± 0.8	0.71 ± 0.06 (1.20)
	V32Fβ	8.4 ± 0.2	0.60 ± 0.02 (1.02)
200	WT	9.8 ± 0.8	0.59 ± 0.03
	A16FJ	7.8 ± 0.6	0.67 ± 0.05 (1.14)
	S28Aβ	7.8 ± 0.1	0.56 ± 0.03 (0.95)
	V32Fβ	7.6 ± 0.4	0.69 ± 0.01 (1.17)

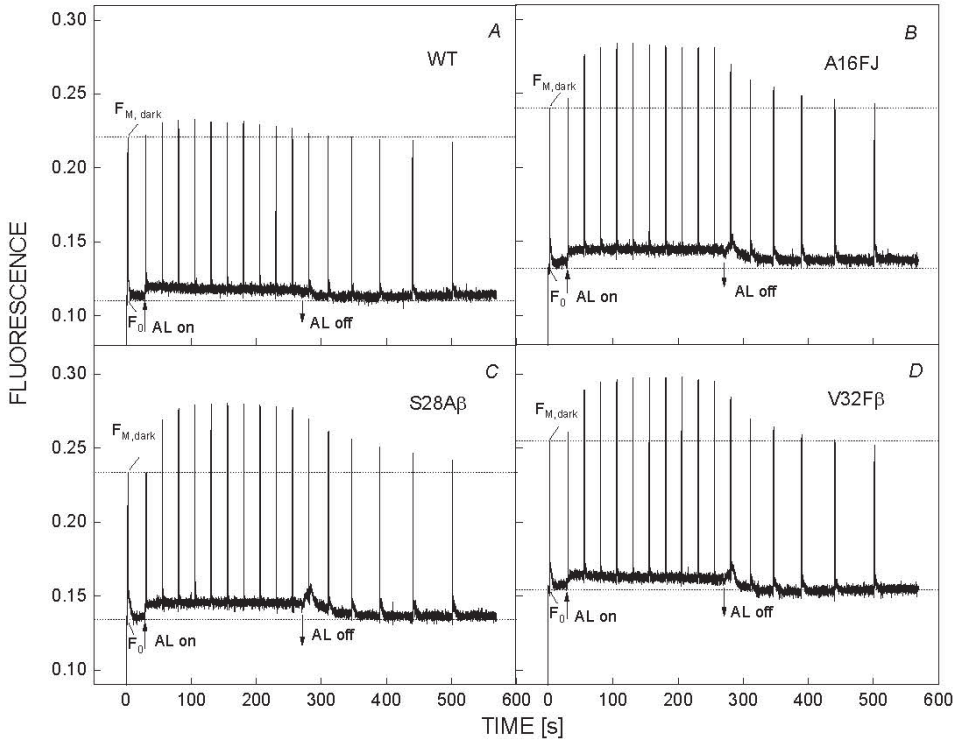

Fig. 2. Time-dependent flash-induced PSII fluorescence yield for WT (*A*), A16FJ (*B*), S28Aβ (*C*), and V32Fβ mutant cells (*D*) with and without low-intensity blue actinic light [light intensity of ~30 μmol(photon) m^{-2} s^{-1}]. WT and mutant cultures were propagated in the photobioreactor under medium-intensity white LED light [~70 μmol(photon) m^{-2} s^{-1}] and 30°C.

a slight increase in PSII fluorescence yield initially (due to the transition to state 1) and then exhibited a weakened effect of blue-light–induced NPQ than that of WT cells (Fig. 3*B–D*). A16FJ, S28Aβ, and V32Fβ mutations on and near the Q_C site in PSII may have a distinct inhibitory effect on OCP-mediated NPQ in mutant cells.

Determination of different potential forms of Cyt b_{559} in WT and mutant PSII core complexes: To estimate the potential forms of Cyt b_{559} in WT and mutant PSII core complexes, we measured reduced minus oxidized optical difference spectra of the Cyt b_{559} heme in WT, S28Aβ, and A16FJ mutant oxygen-evolving PSII core complexes by using four-step titration (Fig. 4). A hydroquinone-reduced minus ferricyanide-oxidized absorption difference spectrum (HF; Fig. 4, dashed line) was used to estimate the high potential (HP) form of Cyt b_{559}, and an ascorbate-reduced minus hydroquinone-oxidized absorption difference spectrum (AH; Fig. 4, thin line) was used to estimate the intermediate potential form of Cyt b_{559}. The dithionite-

reduced minus ascorbate-oxidized absorption difference spectrum (DA; Fig. 4, thick line) of Cyt b_{559} contains both the low-potential (LP) form of Cyt b_{559} and Cyt c_{550}. Because at 559.5 nm, Cyt c_{550} does not contribute significantly to the difference spectrum (Hung *et al*. 2010), we used the amplitude of DA absorption difference spectra at 559.5 nm to estimate the amount of the LP form of Cyt b_{559}. The oxygen-evolving WT PSII core complexes (Fig. 4*A*, Table 2) contained ~7% of the HP form, ~65% of the IP form, and ~28% of the LP form of Cyt b_{559}. The ratios of redox potential forms of Cyt b_{559} were similar for A16FJ and S28Aβ mutant and WT PSII core complexes (Fig. 4 and Table 2), except that the LP form of Cyt b_{559} was slightly higher (~12%) for the S28Aβ mutant than that of WT PSII core complexes. Hence, the structure and redox properties of Cyt b_{559} in A16FJ and S28Aβ mutant PSII core complexes were mostly intact.

Discussion

We found photosynthetic growth rate (the exponential phase) and biomass production greater for most of Q_C-site mutant cells (A16FJ, V32Fβ, and S28Aβ) than that of WT cells under different growth-light conditions [ranging from ~30 μmol(photon) m^{-2} s^{-1} (Huang *et al.* 2016) to ~70 and ~200 μmol(photon) m^{-2} s^{-1} (this study)]. These Q_C-site mutant cells showed significant enhancement of the transition from state 2 to 1 during low-to-medium- intensity

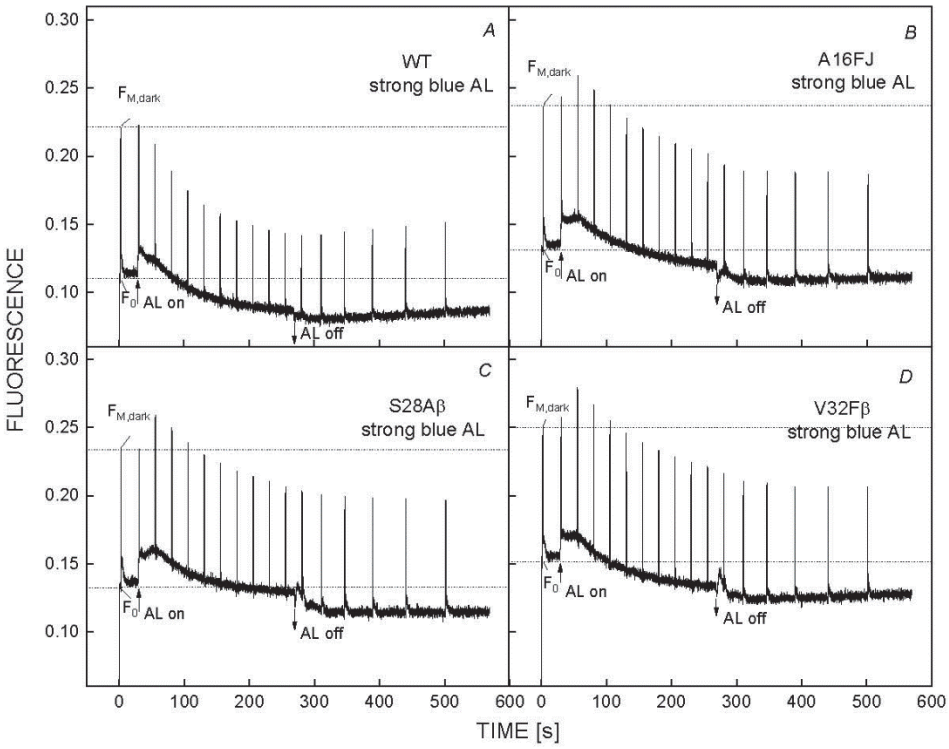

Fig. 3. Time-dependent flash-induced PSII fluorescence yield for WT (*A*), A16FJ (*B*), S28Aβ (*C*), and V32Fβ (*D*) mutant cells with and without high-intensity blue actinic light [light intensity of ~250 μmol(photon) m^{-2} s^{-1}]. WT and mutant cultures were propagated in the photobioreactor under medium-intensity white LED light [~70 μmol(photon) m^{-2} s^{-1}] and 30°C.

blue-light illumination and weakened effects of blue-light–induced NPQ during high-intensity blue-light illumination. Therefore, the increase in photosynthetic growth rate and biomass production in A16FJ, V32Fβ, and S28Aβ mutant cells could be attributed to the decreased dissipation of wasteful energy from phycobilisomes and improved photosynthesis efficiency as compared to WT cells.

In nature, cyanobacteria use diverse photoprotective mechanisms (including state transition and OCP-related NPQ) to prevent the formation of harmful reactive oxygen species and ensure their survival under diverse stress conditions (*e.g.*, light, temperature, nutrients). Because of the trade-offs for photoprotection, photosynthesis in photosynthetic organisms in nature operates below the maximum efficiency. However, in controlled environments, such as growth chambers and photobioreactors, the minimized wasteful energy dissipation from the phycobilisome of cyanobacteria would significantly improve photosynthesis efficiency and biomass production. Our results are consistent with the proposal that manipulation

of photoprotection may improve photosynthesis in photosynthetic organisms (Murchie and Niyogi 2011, Stephenson *et al.* 2011, Kromdijk *et al*. 2016).

Recently, a novel role of Cyt b_{559} in modulating photosynthetic light harvesting in PSII reaction centers of cyanobacteria was proposed. A spontaneously generated R7Lα Cyt b_{559} mutant of *Synechocystis* sp. PCC 6803 outcompeted WT cells under DCMU-inhibited photoheterotrophic conditions (Chiu *et al.* 2009). Data from 77 K fluorescence indicated that the R7Lα mutation of Cyt b_{559} may perturb the energy delivery from the phycobilisomes to PSII and thus protect mutant cells against DCMU-induced photo-oxidative stress. In addition, R7Lα and R17Lβ Cyt b_{559} mutant cells showed significant inhibition of OCP-mediated NPQ under strong blue light illumination and distinct acceleration of its dark recovery (Chiu *et al*. 2013). Thus, the R7Lα and R17Lβ mutations on the cytoplasmic side of Cyt b_{559} may affect the interaction between the phycobilisomes and PSII reaction centers, thereby affecting OCP-mediated NPQ and its dark recovery in mutant cells. Our results generally agree with this proposal, but the Q_C-site mutant cells have some properties that significantly differ from R7Lα and R17Lβ Cyt b_{559} mutant cells (*see* the discussion below).

Previous studies proposed that the Q_C site may be involved in modulating the redox potential and reactivity of Cyt b_{559} (Kruk and Strzałka 1999, 2001, Bondarava *et al*. 2003, Kaminskaya and Shuvalov 2013). From *in silico* structural analysis of the Q_C site in PSIIs of WT and mutant PSIIs, replacing Ala16 residues of PsbJ or Val32 on the beta-subunit of Cyt b_{559} residues with bulky phenylalanine may hinder or block the binding of the PQ molecule to the Q_C site in mutant PSIIs (Huang *et al.* 2016). In addition, the S28β residue of Cyt b_{559} (corresponding to Thr30β residues of Cyt b_{559} in *T. elongatus*) is situated near the opening of the Q_C channel toward the internal space of the thylakoid membranes (Guskov *et al*. 2009, Müh *et al*. 2012). Replacing the Ser28 residue with Ala might hinder the diffusion of the PQ molecules to the Q_C site in mutant PSIIs. Therefore, it needs verification whether these mutations on the Q_C site affect the redox properties and photoptotective function of Cyt b_{559} in mutant PSIIs.

Several early studies suggested that Cyt b_{559} may participate in secondary electron transfer pathways protecting PSII against damaging reactive oxygen species under photoinhibitory conditions (Whitmarsh and Pakrasi 1996, Stewart and Brudvig 1998, Shinopoulos and Brudvig 2012, Chu and Chiu 2015). In addition, prior mutagenesis and biochemical studies suggested possible roles of Cyt b_{559} in assembly and stability of PSII (Pakrasi *et al.* 1988, Morais *et al.* 1998, Komenda *et al.* 2004). For example, R7Lα and R17Lβ mutation on the cytoplasmic side of Cyt b_{559} perturbed the structure of the heme-binding pocket and redox properties of Cyt b_{559} in mutant PSII core complexes. R7Lα and R17Lβ Cyt b_{559} mutant cells showed impaired PSII activities were more susceptible to photoinhibition and grew slower than WT cells under normal growth conditions (Chiu *et al*. 2009, 2013). In contrast, Q_C-site mutant cells (*e.g.*, A16FJ, S28Aβ, and V32Fβ) showed normal PSII activity and grew faster than WT cells under normal growth conditions (Huang *et al.* 2016). In addition, the redox properties of Cyt b_{559} were similar between A16FJ and S28Aβ mutant and WT cells.

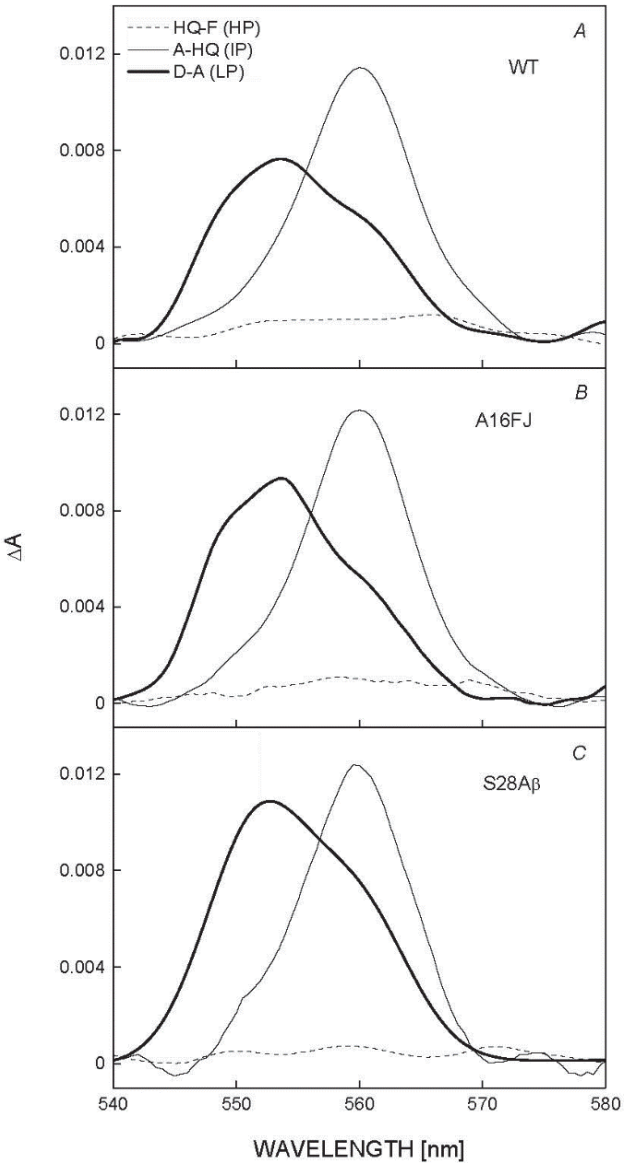

Fig. 4. Reduced minus oxidized difference spectra of Cyt b_{559} heme in oxygen-evolving WT (*A*), S28Aβ (*B*), and A16FJ (*C*) mutant PSII core complexes by using four-step titration. HF, hydroquinone-reduced minus ferricyanide-oxidized difference spectrum (*dashed line*). AH, ascorbate-reduced minus hydroquinone-oxidized difference spectrum (*thin line*). DA, dithionite-reduced minus ascorbate-oxidized difference spectrum (*thick line*). HP, high potential. IP, intermediate potential. LP, low potential.

Table 2. Properties of WT and Q_C-site mutant PSII core complexes. HP – high potential; IP – intermediate potential; LP – low potential. Data are mean ± SD from two independent experiments.

Strain	Oxygen evolution [μmol(O_2) mg^{-1}(Chl) h^{-1}]	Redox potential forms [%] HP	IP	LP
WT	3200 ± 170	7 ± 1	65 ± 1	28 ± 3
S28Aβ	3060 ± 150	2 ± 2	58 ± 2	40 ± 4
A16FJ	2430 ± 60	6 ± 1	64 ± 4	30 ± 3

Several cyanobacteria strains, including *Synechocystis* sp. PCC 6803 and *Synechococcus elongatus* sp. PCC7942, have been used as biofactories for producing biofuels and valuable products (Machado and Atsumi 2012, Al-Haj *et al.* 2016, Gao *et al.* 2016). The genomes of the strains are well characterized, and they are relatively easy to use for genetic engineering. In addition, cyanobacteria are able to capture and convert CO_2 photosynthetically into sugars and other bioproducts, which is an important incentive for using cyanobacteria for production of renewable energy and green chemicals to cope with global warming. Under our experimental conditions [light intensity from ~30 to ~200 μmol(photon) m^{-2} s^{-1}], the improved photosynthesis growth and biomass production of these Q_C-site mutant cells of *Synechocystis* sp. PCC 6803 are intriguing because of their potential applications as biofactories to increase the productivity of biofuels and valuable products. We are applying these Q_C-site mutant cells to more harsh growth conditions (*e.g.,* strong light, high- and low-temperature stress) to explore their potential applications and limitations (Wilhelm and Selmar 2011).

References

Al-Haj L., Lui Y.T., Abed R.M. *et al.*: Cyanobacteria as chassis for industrial biotechnology: progress and prospects. – Life (Basel) **6**: E42, 2016.

Bondarava N., De Pascalis L., Al-Babili S. *et al.*: Evidence that cytochrome b_{559} mediates the oxidation of reduced plasto quinone in the dark. – J. Biol. Chem. **278**: 13554-13560, 2003.

Bondarava N., Gross C.M., Mubarakshina M. *et al.*: Putative function of cytochrome b_{559} as a plastoquinol oxidase. – Physiol. Plantarum **138**: 463-473, 2010.

Boulay C., Wilson A., D'Haene S. *et al.*: Identification of a protein required for recovery of full antenna capacity in OCP-related photoprotective mechanism in cyanobacteria. – P. Natl. Acad. Sci. USA **107**: 11620-11625, 2010.

Bruce D., Brimble S., Bryant D.A.: State transitions in a phycobilisome-less mutant of the cyanobacterium *Synechococcus* sp. PCC 7002. – Biochim. Biophys. Acta **974**: 66-73, 1989.

Chiu Y.F., Chen Y.H., Roncel M. *et al.*: Spectroscopic and functional characterization of cyanobacterium *Synechocystis* PCC 6803 mutants on the cytoplasmic-side of cytochrome b_{559} in photosystem II. – Biochim. Biophys. Acta **1827**: 507-519, 2013.

Chiu Y.F., Lin W.C., Wu C.M. *et al.*: Identification and characterization of a cytochrome b_{559} *Synechocystis* 6803 mutant spontaneously generated from DCMU-inhibited photoheterotrophical growth conditions. – Biochim. Biophys. Acta **1787**: 1179-1188, 2009.

Chu H.A., Chiu Y.F.: The roles of cytochrome b_{559} in assembly and photoprotection of photosystem II revealed by site-directed mutagenesis studies. – Front. Plant Sci. **6**: 1261, 2015.

Gao X., Sun T., Pei G. *et al.*: Cyanobacterial chassis engineering for enhancing production of biofuels and chemicals. – Appl. Microbiol. Biotechnol. **100**: 3401-3413, 2016.

Guskov A., Kern J., Gabdulkhakov A. *et al.*: Cyanobacterial photosystem II at 2.9-Å resolution and the role of quinones, lipids, channels and chloride. – Nat. Struct. Mol. Biol. **16**: 334-342, 2009.

Hasegawa K., Noguchi T.: Molecular interactions of the quinone electron acceptors Q_A, Q_B, and Q_C in photosystem II as studied by the fragment molecular orbital method. – Photosynth. Res. **120**: 113-123, 2014.

Huang J.Y., Chiu Y.F., Ortega J.M. *et al.*: Mutations of cytochrome b_{559} and psbJ on and near the Q_C Site in photosystem II influence the regulation of short-term light response and photosynthetic growth of the cyanobacterium *Synechocystis* sp. PCC 6803. – Biochemistry **55**: 2214-2226, 2016.

Hung C.H., Huang J.Y., Chiu Y.F. *et al.*: Site-directed mutagenesis on the heme axial-ligands of cytochrome b_{559} in photosystem II by using cyanobacteria *Synechocystis* PCC 6803. – Biochim. Biophys. Acta **1767**: 686-693, 2007.

Hung C.H., Hwang H.J., Chen Y.H. *et al.*: Spectroscopic and functional characterizations of cyanobacterium *Synechocystis* PCC 6803 mutants on and near the heme axial ligand of cytochrome b_{559} in photosystem II. – J. Biol. Chem. **285**: 5653-5663, 2010.

Kaminskaya O., Shuvalov V.A., Renger G.: Evidence for a novel quinone-binding site in the photosystem II (PS II) complex that regulates the redox potential of cytochrome b_{559}. – Biochemistry **46**: 1091-1105, 2007a.

Kaminskaya O., Shuvalov V.A., Renger G.: Two reaction pathways for transformation of high potential cytochrome b_{559} of PS II into the intermediate potential form. – BBA-Bioenergetics **1767**: 550-558, 2007b.

Kaminskaya O.P., Shuvalov V.A.: Biphasic reduction of cytochrome b_{559} by plastoquinol in photosystem II membrane fragments: evidence for two types of cytochrome b_{559}/plastoquinone redox equilibria. – BBA-Bioenergetics **1827**: 471-483, 2013.

Kirilovsky D.: Modulating energy arriving at photochemical reaction centers: orange carotenoid protein-related photoprotection and state transitions. – Photosynth. Res. **126**: 3-17, 2015.

Kirilovsky D., Kerfeld C.A.: Cyanobacterial photoprotection by the orange carotenoid protein. – Nat. Plants **2**: 16180, 2016. doi: 10.1038/nplants.2016.180

Komenda J., Reisinger V., Müller B.C. *et al.*: Accumulation of the D2 protein is a key regulatory step for assembly of the photosystem II reaction center complex in *Synechocystis* PCC 6803. – J. Biol. Chem. **279**: 48620-48629, 2004.

Kondo K., Mullineaux C.W., Ikeuchi M.: Distinct roles of

CpcG1-phycobilisome and CpcG2-phycobilisome in state transitions in a cyanobacterium *Synechocystis* sp. PCC 6803. – Photosynth. Res. **99**: 217-225, 2009.

Kromdijk J., Głowacka K., Leonelli L. *et al.*: Improving photosynthesis and crop productivity by accelerating recovery from photoprotection. – Science **354**: 857-861, 2016.

Kruk J., Strzałka K.: Redox changes of cytochrome b_{559} in the presence of plastoquinones. – J. Biol. Chem. **276**: 86-91, 2001.

Kruk J., Strzałka K.: Dark reoxidation of the plastoquinone-pool is mediated by the low-potential form of cytochrome b_{559} in spinach thylakoids. – Photosynth. Res. **62**: 273-279, 1999.

Machado I.M., Atsumi S.: Cyanobacterial biofuel production. – J. Biotechnol. **162**: 50-56, 2012.

Morais F., Barber J., Nixon P.J.: The chloroplast-encoded alpha subunit of cytochrome b_{559} is required for assembly of the photosystem two complex in both the light and the dark in *Chlamydomonas reinhardtii*. – J. Biol. Chem. **273**: 29315-29320, 1998.

Müh F., Glöckner C., Hellmich J. *et al.*: Light-induced quinone reduction in photosystem II. – Biochim. Biophys. Acta **1817**: 44-65, 2012.

Mullineaux C.W., Allen J.F.: State 1-State 2 transitions in the cyanobacterium *Synechococcus* 6301 are controlled by the redox state of electron carriers between Photosystems I and II. – Photosynth. Res. **23**: 297-311, 1990.

Murchie E.H., Niyogi K.K.: Manipulation of photoprotection to improve plant photosynthesis. – Plant Physiol. **155**: 86-92, 2011.

Page L.E., Liberton M., Pakrasi H.B.: Reduction of photoautotrophic productivity in the cyanobacterium *Synechocystis* sp. strain PCC 6803 by phycobilisome antenna truncation. – Appl. Environ. Microbiol. **78**: 6349-6351, 2012.

Pakrasi H.B., Williams J.G., Arntzen C.J.: Targeted mutagenesis of the psbE and psbF genes blocks photosynthetic electron transport: evidence for a functional role of cytochrome b_{559} in photosystem II. – EMBO J. **7**: 325-332, 1988.

Shinopoulos K.E., Brudvig G.W.: Cytochrome b_{559} and cyclic electron transfer within photosystem II. – Biochim. Biophys. Acta **1817**: 66-75, 2012.

Stephenson P.G., Moore C.M., Terry M.J. *et al.*: Improving photosynthesis for algal biofuels: toward a green revolution. – Trends Biotechnol. **29**: 615-623, 2011.

Stewart D.H., Brudvig G.W.: Cytochrome b_{559} of photosystem II. – BBA-Bioenergetics **1367**: 63-87, 1998.

Suga M., Akita F., Hirata K. *et al.*: Native structure of photosystem II at 1.95 Å resolution viewed by femtosecond X-ray pulses. – Nature **517**: 99-103, 2015.

Umena Y., Kawakami K., Shen J.R. *et al.*: Crystal structure of oxygen-evolving photosystem II at a resolution of 1.9 Å. – Nature **473**: 55-60, 2011.

Whitmarsh J., Pakrasi H.B.: Form and function of cytochrome b_{559}. – In: Ort D.R., Yocum C.F., Heichel I.F. (ed.): Oxygenic photosynthesis: The Light Reactions. Pp. 249-264. Springer, Dordrecht 1996.

Wilhelm C., Selmar D.: Energy dissipation is an essential mecha nism to sustain the viability of plants: The physiological limits of improved photosynthesis. – J. Plant Physiol. **168**: 79-87, 2011.

Wilson A., Ajlani G., Verbavatz J.M. *et al.*: A soluble carotenoid protein involved in phycobilisome-related energy dissipation in cyanobacteria. – Plant Cell **18**: 992-1007, 2006.